Annihilation of Angular Momentum Bias and Velocity Pointing Errors

Victor Gandarillas* *Purdue University, West Lafayette, IN 47906*

This paper is the reproduction of two previous papers, [1] and [2]. In addition to reproducing the results, the assumption that a spacecraft be rotating about a stable principal axis is tested for the two burn scheme and it is shwon that the trapeziodal thrust scheme works for non axisymmetric bodies. The annihilation of angular momentum bias through the two burn scheme is shown to work and the trapezoidal thrust scheme is shown to reduce velocity pointing errors dramatically. The Galileo spacecraft and STAR 48B Payload Assist Module are used in this work.

I. Introduction

In order to provide stability, rockets and spacecraft are usually spun up. Due to thruster misalignments, introducing a torque not only increases spin rate, but also changes the angular momentum vector (Fig. 1). The angular momentum vector **H** traces a circular path in inertial space. The average orientation of **H** is given by the angle ρ_0, which is in the YZ plane.

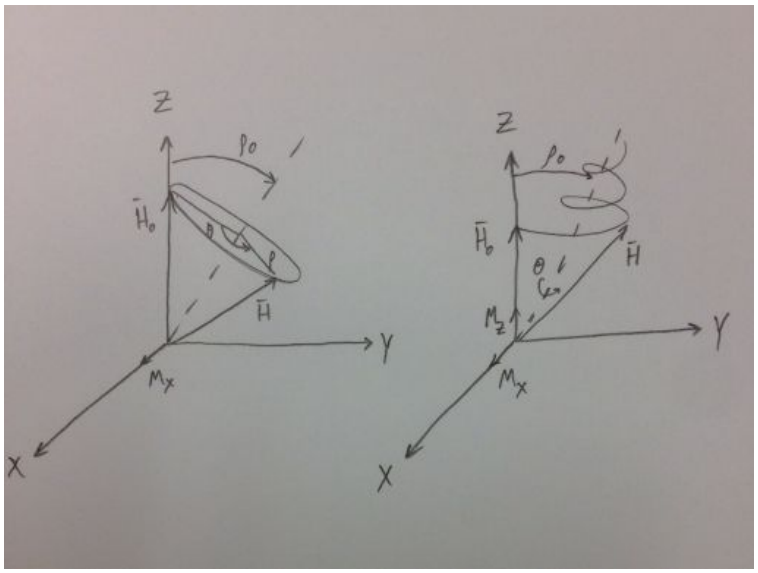

Figure 1. Angular momentum for spinup maneuver, thrusting (left) and spinning up (right) (reproduced based on Longuski, Kia, and Breckenridge [1])

Ideally, only axial torques should be applied to the spacecraft, but thruster misalignments cause the angular momentum vector to shift in space. By breaking up the spin up maneuver into two burns with a coast in between, the velocity pointing error is eliminated by making **H** rotate about the Z axis.

The trapezoid scheme is also analyzed to eliminate pointing errors. A schematic of this maneuver is shown in Fig. 2 below.

*Undergraduate Student, Department of Aeronautics and Astronautics, AIAA Student Member, vgandari@purdue.edu

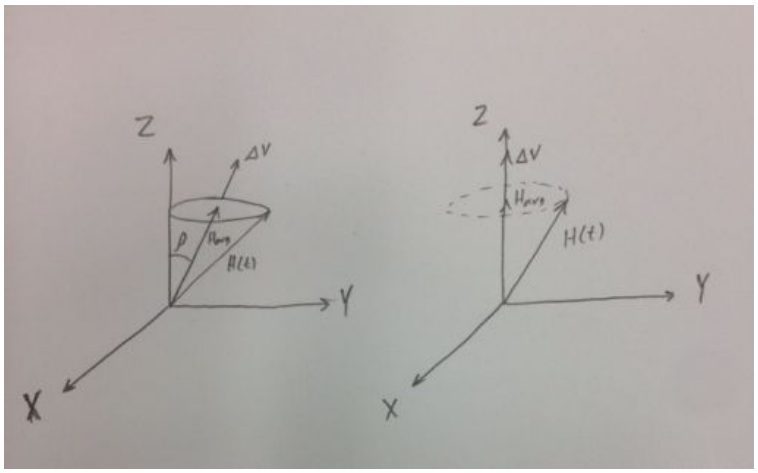

Figure 2. Angular momentum for trapezoid thrust profile scheme, constant torque (left) and increasing torque (right) (reproduced based on Longuski, Kia, and Breckenridge [1])

II. Analytic Solutions

The spacecraft follows Euler's law,

$$M = \dot{H} \tag{1}$$

The spin rate Ω is assumed constant for the two burn scheme and the body-fixed torques are fixed in the body. Then equation (1) becomes (from [1])

$$\dot{H}_X = M_X = M_x \cos\Omega t - M_y \sin\Omega t \tag{2}$$

$$\dot{H}_Y = M_Y = M_x \sin\Omega t - M_x \cos\Omega t \tag{3}$$

$$\dot{H}_Z = 0 \tag{4}$$

Equations (2-4) are then integrated to become

$$H_X = (M_x/\Omega)\cos\Omega t - M_y \sin\Omega t \tag{5}$$

$$H_Y = (M_x/\Omega)\sin\Omega t - M_x \cos\Omega t \tag{6}$$

$$H_Z = 0 \tag{7}$$

As in [1, 2], a 3-1-2 Euler Angle sequence [5] is used and the following dynamic and kinematic equations of motion are integrated:

$$M_x = I_x\dot{\omega}_x + (I_z - I_y)\omega_y\omega_z \tag{8}$$

$$M_y = I_y\dot{\omega}_y + (I_x - I_z)\omega_z\omega_x \tag{9}$$

$$M_z = I_z\dot{\omega}_z + (I_y - I_x)\omega_x\omega_y \tag{10}$$

$$\dot{\phi}_x = \omega_x \cos\phi_y + \omega_z \sin\phi_y \tag{11}$$

$$\dot{\phi}_y = \omega_y - (\omega_z \cos\phi_y - \omega_x \sin\phi_y)\tan\phi_x \tag{12}$$

$$\dot{\phi}_z = \omega_y - (\omega_z \cos\phi_y - \omega_x \sin\phi_y)\sec\phi_x \tag{13}$$

The solutions for H is

$$\begin{bmatrix} H_X \\ H_y \\ H_Z \end{bmatrix} = \begin{bmatrix} c\phi_z c\phi_y - s\phi_z s\phi_x s\phi_y & -s\phi_z c\phi_x & c\phi_z c\phi_y + s\phi_z s\phi_x c\phi_y \\ s\phi_z c\phi_y + c\phi_z s\phi_x s\phi_y & c\phi_z c\phi_x & s\phi_z s\phi_y - c\phi_z c\phi_x c\phi_y \\ -c\phi_x s\phi_y & s\phi_x & c\phi_x c\phi_y \end{bmatrix} \begin{bmatrix} I_x\omega_x \\ I_y\omega_y \\ I_z\omega_z \end{bmatrix} \tag{14}$$

where s and c correspond to sine and cosine, respectively.

A very accurate approximate analytic solution is given by equation (15) [1, 3]

$$\begin{bmatrix} H_X \\ H_y \\ H_Z \end{bmatrix} = \begin{bmatrix} c\phi_z & -s\phi_z & phi_y c\phi_z + \phi_x s\phi_z \\ s\phi_z & c\phi_z & \phi_y s\phi_z - \phi_x c\phi_z \\ -\phi_y & \phi_x & 1 \end{bmatrix} \begin{bmatrix} I_x\omega_x \\ I_y\omega_y \\ I_z\omega_z \end{bmatrix} \tag{15}$$

The angluar momenta are calculated based on simulation data using equation (15) and presented in all subsequent plotsh as suc.

III. Two Burn Scheme Numerical Results

For the two burn scheme, the thrusting spin up maneuver is shown in Fig. 3. There is a first burn, followed by a coasting period where the angular momentum vector is stationary, and a second burn, where the angular momentum follows the path of a circle about the origin if there is a moment in only the X or Y direction. The plot shown here is for the Galileo spacecraft with $M = -0.4757, -0.5669, 13^T$ Nm and $I_x = 3012kg - m^2, I_y = 2761kg - m^2, I_z = 5106kg - m^2$ [6].

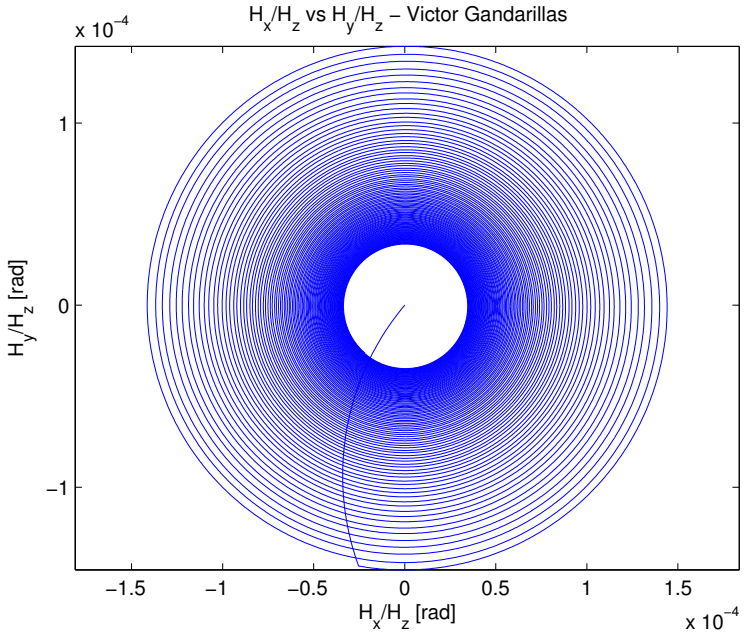

Figure 3. Angular momentum for two burn scheme about largest PMOI, thrusting and spinning up (reproduced based on Longuski, Kia, and Breckenridge [1])

Fig. 3 corresponds to a spin up about Galileo's largest principal moment of inertia (PMOI). The distance from the origin to any point on the spiral can be approximated by [1, 4]

$$\rho(t) = (M_x^2 + M_y^2)^{1/2}/I_z\omega_z^2(t) \tag{16}$$

It is assumed that the spacecraft is always spun up about a stable principal moment of inertia. The velocity pointing error is given by equations (16)-(19) below [1].

$$\Delta V_X = (f_z/m)[\phi_{y0} + I_x\omega_{x0}(I_z\Omega)^{-1} - M_y(I_z\Omega^2)^{-1}]t \tag{17}$$

$$\Delta V_Y = (f_z/m)[-\phi_{x0} + I_y\omega_{y0}(I_z\Omega)^{-1} - M_x(I_z\Omega^2)^{-1}]t \tag{18}$$

$$\Delta V_Z = (f_z/m)[1 - (f_x/f_z)M_y(I_z - Ix)^{-1}\Omega^{-2} + (f_y/f_z)M_x(I_z - Iy)^{-1}\Omega^{-2}]t \tag{19}$$

The velocity pointing error for the two burn scheme about the largest PMOI is shown in Fig. 4.

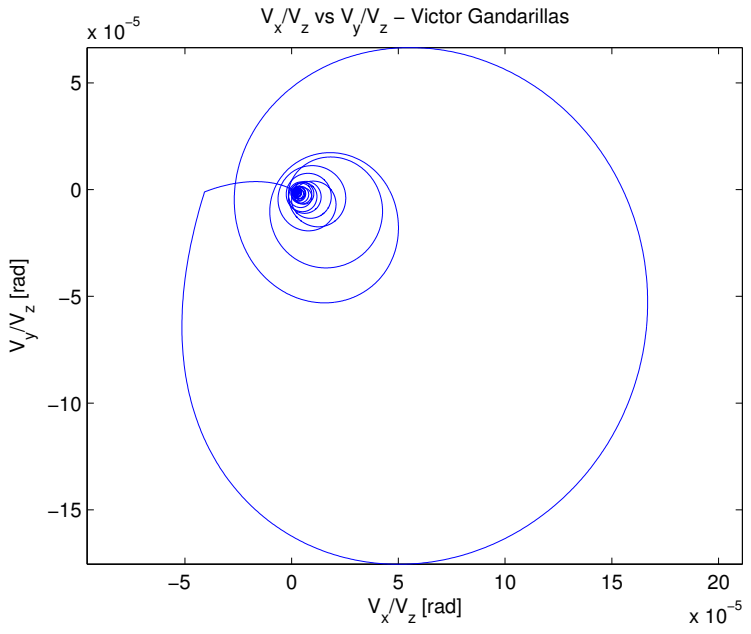

Figure 4. Velocity pointing error for two burn scheme about largest PMOI, thrusting and spinning up

The motion of he spacecraft is also stable for the smallest PMOI, as shown in Fig. 5 and 6

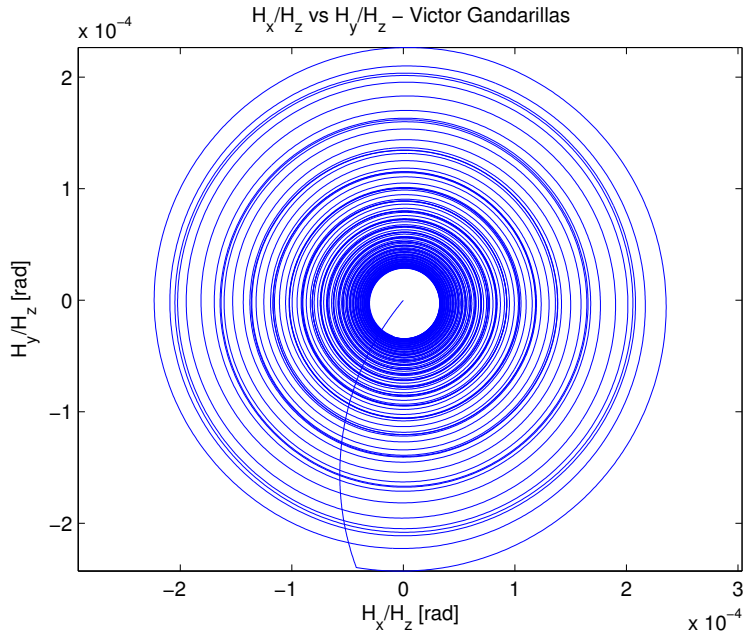

Figure 5. Angular Momentum for two burn scheme about smallest PMOI, thrusting and spinning up

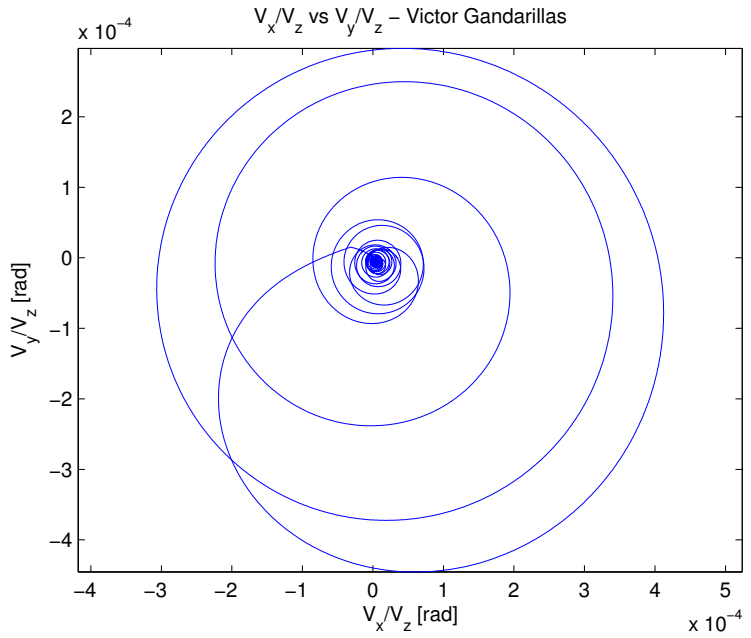

Figure 6. Velocity pointing error for two burn scheme about smallest PMOI, thrusting and spinning up

Spinning about the intermetiate PMOI, the spacecraft becomes unstable, as shown in Fig. 7. Note that the velocity pointing error is not guaranteed to decay as with the stable spinup. At best, the velocity error remains bounded, but does not approch zero asymptotically.

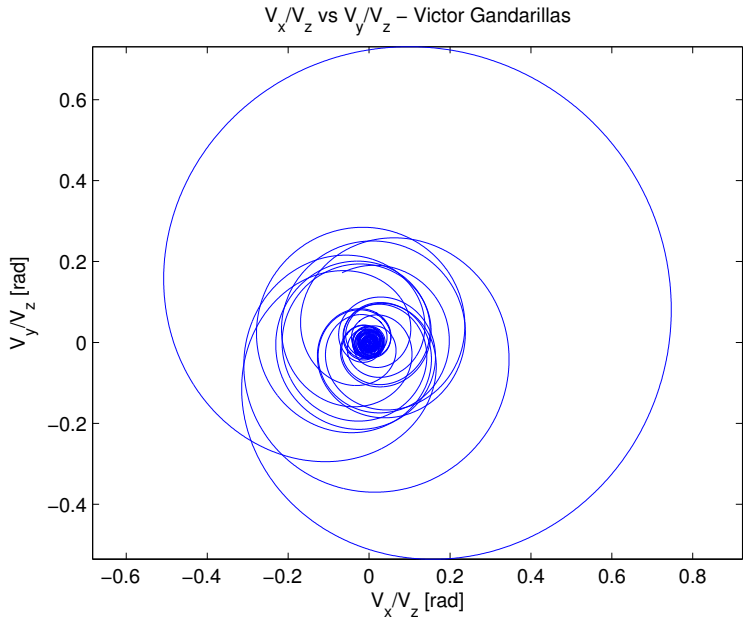

Figure 7. Velocity pointing error for two burn scheme about intermediate PMOI, thrusting and spinning up

The two burn scheme for time varying PMOI is shown in Fig. 8 below.

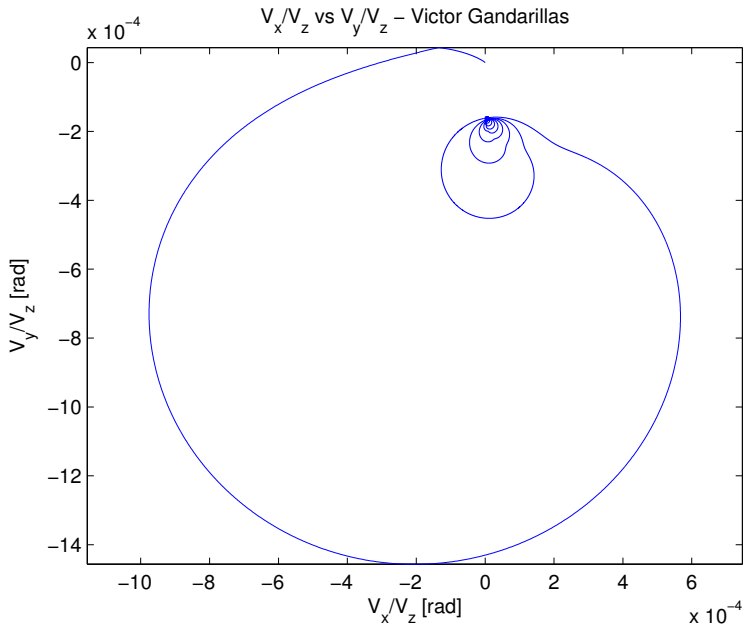

Figure 8. Velocity pointing error for two burn scheme about largest PMOI with decreasing moments of inertia; pointing error grows initially with time

The velocity error increases with time during the two burn scheme for time-varying moments of inertia. The trapezoidal thrust profile scheme is better suited for varying PMOI.

IV. Trapezoidal Thrust Scheme

Teh trapezoidal thrust profile is the same as in [2]. The thrust during the ramp up and ramp down phases increases and decreases linearly with time. The PMOI are assumed to remain constant during phase I (ramp up) and phase II (ramp down), but decrease linearly with time during phase II [2]. The solution can be found using Fresnel integrals [3]. The Fresnel functions can be approximated by [7, 8]

$$C(z) = \frac{1}{2} + f(z)\sin(\frac{pi}{2}z^2) - g(z)\cos(\frac{pi}{2}z^2) \tag{20}$$

$$S(z) = \frac{1}{2} - f(z)\cos(\frac{pi}{2}z^2) - g(z)\sin(\frac{pi}{2}z^2) \tag{21}$$

$$f(z) = \frac{1 + 0.926z}{2 + 1.792z + 3.104z^2} + \varepsilon(z) \tag{22}$$

$$g(z) = \frac{1}{2 + 4.142z + 3.492z^2 + 6.670z^3} + \varepsilon(z) \tag{23}$$

$$|\varepsilon(z)| \leq 2 \times 10^{-3} \tag{24}$$

The analytic soltuions for the trapezoidal scheme are given by equations (25)-(36) [2] Phase 1, $t < t_{r0}$:

$$H_X = (h_0 \sin\alpha + d\cos\alpha)(F_{max}/t_{r0}\Omega_0)[(1/\Omega_0)\cos(\Omega_0 t) + 1\sin(\Omega_0 t) - 1/\Omega_0] \tag{25}$$

$$H_Y = (h_0 \sin\alpha + d\cos\alpha)(F_{max}/t_{r0}\Omega_0)[(1/\Omega_0)\sin(\Omega_0 t) - 1\cos(\Omega_0 t) \tag{26}$$

$$H_Z = I_{Z0}\Omega_0 \tag{27}$$

Phase II, $t_{r0} < t < t_{rf}$:

$$H_X = M_{xmax} sqrt \frac{\pi}{a}\left[\cos(\tfrac{\Omega_0^2}{2a})C(z) + \sin(\tfrac{\Omega_0^2}{2a})S(z)\right] \tag{28}$$

$$H_Y = M_{xmax} sqrt \frac{\pi}{a}\left[\cos(\tfrac{\Omega_0^2}{2a})S(z) - \sin(\tfrac{\Omega_0^2}{2a})C(z)\right] \tag{29}$$

$$H_Z = I_{Z0}\Omega_0 \tag{30}$$

where

$$M_{xmax} = F_{max}(h_{avg}\sin\alpha + \cos\alpha) \tag{31}$$

$$a = \frac{\Omega_0}{t_b - t_{r0} - t_{rf}}(\frac{I_{z0}}{I_{zf}} - 1) \tag{32}$$

$$z = sqrt\frac{4}{a\pi}\left[\frac{a(t-t_{r0})+\Omega_0}{2}\right] \tag{33}$$

Phase 3, $t_b - t_{rf} < t < t_b$:

$$H_X = (h_f\sin\alpha + d\cos\alpha)(F_{max}/t_{rf}\Omega_f)[(1/\Omega_f)\cos(\Omega_f t) + 1\sin(\Omega_f t) - 1/\Omega_f] \tag{34}$$

$$H_Y = (h_f\sin\alpha + d\cos\alpha)(F_{max}/t_{rf}\Omega_f)[(1/\Omega_f)\sin(\Omega_f t) - 1\cos(\Omega_f t) \tag{35}$$

$$H_Z = I_{Zf}\Omega_f \tag{36}$$

The angluar momentum equations only depend on th axial moment of inertia, and not on any other moment of inertia. The numerical simulations agree with this assumption. Ther eis also no effect of the symmetry of the spacecraft on the stability of the motion.

The trapezoidal trhust scheme from [2] was tested with data from [9]. Fig. 9-11 show the three phases of ramp up, constant thrust, and ramp down.

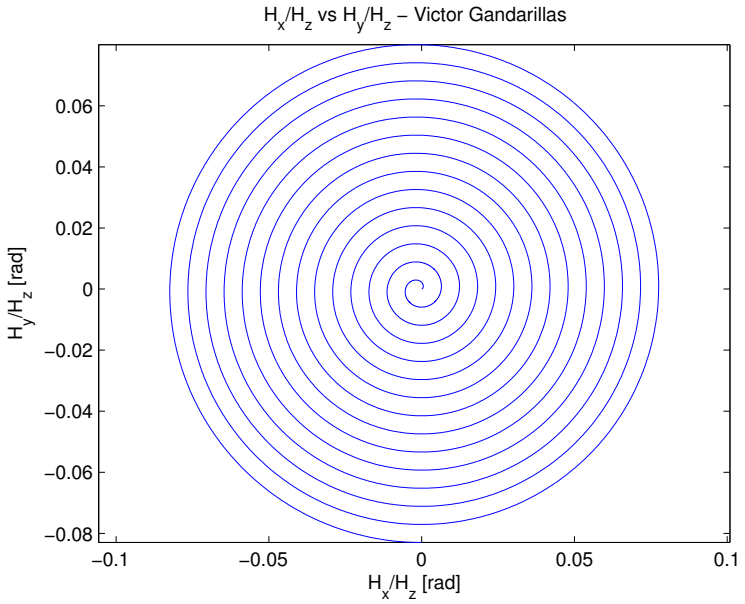

Figure 9. Angular momentum during phase I of trapzoid thrust profile scheme (reproduced based on Javorsek II, Longuski [2])

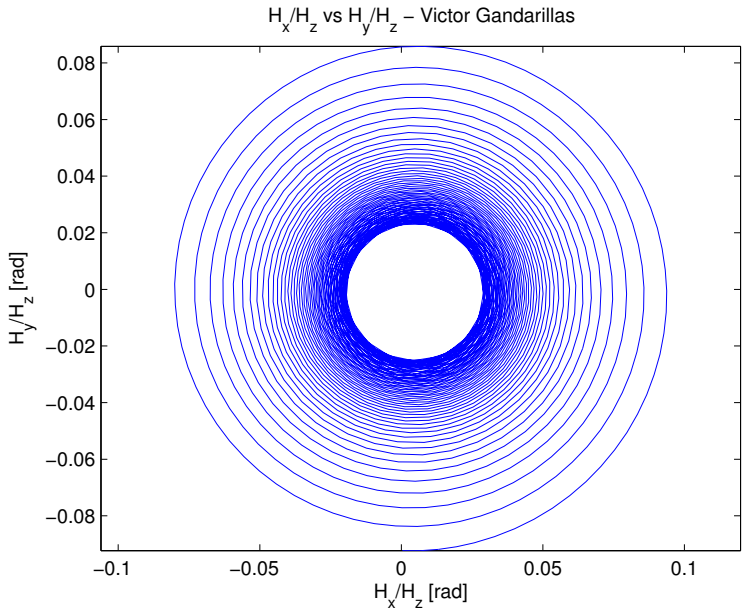

Figure 10. Angular momentum during phase II of trapzoid thrust profile scheme (reproduced based on Javorsek II, Longuski [2])

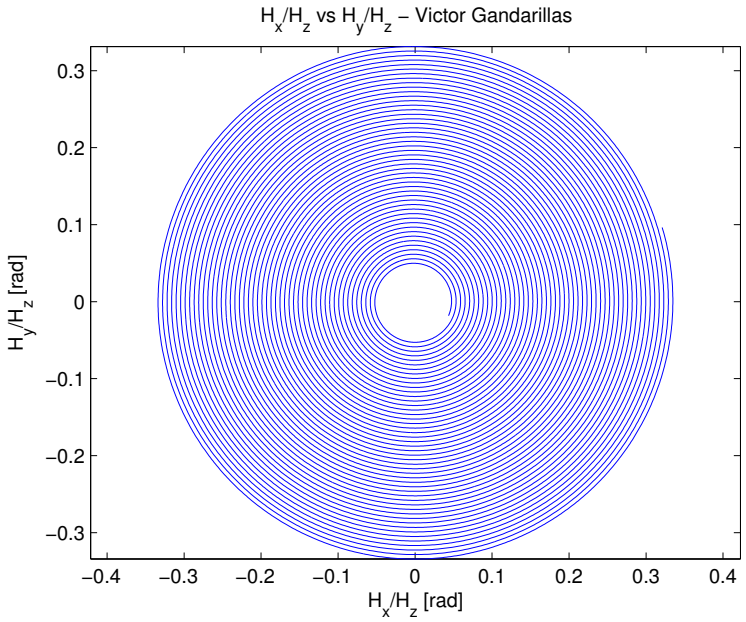

Figure 11. Angular momentum during phase III of trapzoid thrust profile scheme (reproduced based on Javorsek II, Longuski [2])

V. Conclusions

1. The two burn scheme has been reproduced from [1]. The velocity pointing error has been reduced and the angular momentum drift has been annihilated using this scheme.

2. Furthermore, the assumption that the body must spin about a stable principal axis has been tested and shown that the two burn scheme does not work for spinning about the intermediate axis, as this is the naturally unstable axis.

3. The velocity pointing error can be approximated by the average orientation of the angular momentum vector in

inertial space, reproduced here from [2].

4. Velocity pointing error can be reduced using a trapexoidal thrust profile, closely matching a solid rocket engine.

5. In addition to allowing for a lower spin rate for a given velocity pointing error, the trapezoidal thrust scheme works regardless of whether or not the body is symmetrtic.

6. The two burn scheme is suitable for use with liquid fuel rockets, where the thrusters can be turned on and off, whereas the trapezoidal thrust profile scheme is suitable for solid rocket motors, where the thrust ends to spike at startup and shutdown. the trapezoidal scheme is also better for taking into account changes in PMOI.

References

[1] Longuski, J.M., Kia, T. and Breckenridge, W.G., "Annihilation of Angular Momentum Bias During Thrusting and Spinning-Up Maneuvers," *Journal of the Astronautical Sciences*, Vol. 37, No. 4, 1989, pp. 433-450.

[2] Javorsek II, D., Longuski, J.M., "Velocity Pointing Errors Associated with Spinning Thrusting Spacecraft," *Journal of Spacecraft and Rockets*, Vol. 37, No. 3, May-June 2000.

[3] Longuski, J.M, "Solution of Euler's Equations of Motion and Eulerian Angles for Near Symmetric Rigin Bodies Subject to Constant Moments," AIAA Paper 80-1642, AIAA/AAS Astrodynamics Conference, Danvers, Massachussetts, August 11-13, 1980.

[4] Kia, T.and Longuski, J.M. "Error Analysis of Analytic Solutions for Self-Excited Near symmetric Rigid Bodies: A Numerical Study," AIAA Paper 84-2081, AIAA/AAS Astrodyamics Conference, Seattle, Washington, August 20-22, 1984.

[5] Wertz, J.R. *Spacecraft Attitude Determination and Control*, D. Reidel Publishing Company, Dordrecht, Holland, 1980.

[6] Longuski, J.M. "Galileo Maneuver Analysis," Paper No. 81-137, AAS/AIAA Astrodyamics Conference, Lake Tahoe, Nevada, August 3-5, 1981.

[7] Abramowitz, M. and Stegun, I. *Handbook of Mathematical Functions*, Dover Publucations, Inc. New York, December 1972.

[8] Boersma, J., "Computation of Fresnel Integrals," *Mathematics of Computation*, Vol. 14, No. 72, 1960, p. 380.

[9] Jaffe, P., Diner, A. Mc Ronald, A., and Tenn, L., "Breakup Analysis Final Report," Jet Propulsion Laboratory, D-1968, 1628-54, California Institute of Technology, Pasadena, California, Nov. 1984.